INTERNATIONAL JOURNAL FOR NUMERICAL METHODS IN FLUIDS
Int. J. Numer. Meth. Fluids 2008; **56**:927–940
Published online 17 July 2007 in Wiley InterScience (www.interscience.wiley.com). DOI: 10.1002/fld.1559

Solutions of slow Brinkman flows using the method of fundamental solutions

C. C. Tsai*, †

Department of Information Technology, Toko University, Chia-Yi County 61363, Taiwan

SUMMARY

This paper develops the method of fundamental solutions (MFS) as a meshless numerical method to obtain solutions of two- and three-dimensional slow Brinkman-extended Darcy's flows. The solutions of the steady Brinkman equations are obtained by utilizing the boundary collocation method as well as the expansion of the fundamental solutions, which are derived by using the Hörmander operator decomposition technique. All the velocities, their partial derivatives, the pressure, and the stresses corresponding to the fundamental solutions are addressed explicitly in tensor forms. Two- and three-dimensional Brinkman problems with Dirchlet and Robin boundary conditions are carried out to validate the proposed numerical schemes. Then, the method is applied to solve a peanut-shaped problem and a joint flow of Stokes and Brinkman fluids. In the spirits of MFS, the proposed numerical scheme is free from singularities and numerical integrations and it also does not require any domain discretization. Copyright © 2007 John Wiley & Sons, Ltd.

Received 23 February 2007; Revised 18 May 2007; Accepted 27 May 2007

KEY WORDS: meshless; method of fundamental solutions; Brinkman equation; porous media; Stokes flow

1. INTRODUCTION

The transport phenomena in porous media arise in many diverse fields of science and engineering, such as civil, mechanical, chemical, and petroleum engineering. A porous medium is defined by a material consisting of a solid matrix with interconnected voids filled with fluids. The porous media can be either naturally formed or fabricated. Thus, the analysis of transport phenomena in porous media is of great importance in science and engineering.

The original works on the porous media dated back to the studies of Darcy [1] in 1856. Thereafter, the transport phenomena in porous media had been studied extensively over years [2–6]. Most of

*Correspondence to: C. C. Tsai, Department of Information Technology, Toko University, Chia-Yi County 61363, Taiwan.
†E-mail: tsaichiacheng@ntu.edu.tw

Contract/grant sponsor: National Science Council of Taiwan; contract/grant number: NSC 95-2221-E-464-002

these studies are based on the Brinkman extended Darcy's model [2]. Tam [7] demonstrated that a viscous fluid flowing through a cloud of spherical particles could be theoretically reduced to a problem governed by the Brinkman equation. Lundgren [8] and Howells [9] also found similar reductions on theoretical grounds for fluids flowing through random arrays of spheres and parallel circular posts, respectively.

Although analytical treatments have been applied to obtain solutions of Brinkman equation [10], their usages are usually limited to canonical domains. Numerical methods are thus applied to obtain solutions for arbitrary domains. In the last few decades, researchers have paid attention to the meshless numerical methods without employing the concept of element. In this paper, we consider the application of the method of fundamental solutions (MFS) which is a boundary-type meshless numerical method. The MFS was first proposed by Kupradze and Aleksidze [11]. Its mathematical foundations were established by Mathon and Johnston [12] and Bogomolny [13]. Then, the MFS was successfully applied to the elliptic boundary value problems [14], the scattering and radiation problems [15], the evaluation of eigenvalues [16], and the diffusion problems [17].

The MFS has also been applied to solve problems of fluid flows. Tsai *et al*. [18] obtained the solution of the three-dimensional Stokes problems by utilizing the combination of the dual reciprocity method as well as the MFS based on the Laplace and modified Helmholtz fundamental solutions. On the other hand, Alves and Silvestre [19] and Tsai *et al*. [20] applied the MFS based on the Stokeslet for interior and exterior Stokes flow problems, respectively. In this paper, we extend the previous studies to the Brinkman equations by using the fundamental solutions of Brinkman equations. Furthermore, we consider a joint flow of Stokes and Brinkman fluids.

When time-dependent problems are solved by the MFS, they are treated either by the time-dependent fundamental solutions [17] or by the finite difference or Laplace transform in time [21]. When the unsteady Stokes problems were solved by the former method, the accuracy was sensitive with respect to the locations of sources [22]. On the other hand, Brinkman equations are deduced if the finite difference or Laplace transform is carried out to deal with time derivatives of the unsteady Stokes equations. Thus, the present study can also be viewed as a preliminary work to solve unsteady Stokes or even Navier–Stokes problems.

Overall, this paper develops the MFS as a meshless numerical method to solve Brinkman equations. Furthermore, it avoids the problems of singularities by addressing the sources of the fundamental solutions on a fictitious curve (surface for three dimensional) outside the computational domain and simply collocates the boundary conditions without integration. The contents of this paper are organized as following: the governing equations and the corresponding fundamental solution are revisited in Section 2. Then, the MFS formulations are introduced in Section 3 and the validation of the present numerical scheme as well as the numerical results for various Brinkman problems are delineated in Section 4. Finally, the main conclusions of the present study are drawn in Section 5.

2. GOVERNING EQUATIONS AND THEIR FUNDAMENTAL SOLUTIONS

For a slow Brinkman-extended Darcy's flow, the mass and momentum conservation equations are given by [2]:

$$\begin{aligned} \nabla \cdot \mathbf{u} &= 0 \\ -\nabla p + \mu \nabla^2 \mathbf{u} &= \frac{\mu}{\kappa} \mathbf{u} \end{aligned} \quad \text{in } \Omega \tag{1}$$

DOI: 10.1002/fld

where $\mathbf{u}=(u_1, u_2, u_3)$ is the velocity, p is the pressure, μ is the viscosity, and κ is the permeability. To form a well-posed problem, proper boundary conditions should be imposed:

$$\begin{aligned} \mathbf{u} &= \overline{\mathbf{u}} \quad \text{on } \Gamma_1 \\ \mathbf{t} &= \overline{\mathbf{t}} \quad \text{on } \Gamma_2 \end{aligned} \tag{2}$$

where $\overline{\mathbf{u}}$ and $\overline{\mathbf{t}}$ are prescribed boundary data, and $\Gamma=\Gamma_1+\Gamma_2$ is the boundary of the computational domain Ω. In addition, $\mathbf{t}=(t_1, t_2, t_3)$ is the traction boundary condition defined by

$$t_i = \sigma_{ij} n_j \tag{3}$$

where $\mathbf{n}=(n_1, n_2, n_3)$ is the outward normal vector and σ_{ij} is the stress tensor defined by

$$\sigma_{ij} = -p + \mu\left(\frac{\partial u_i}{\partial x_j} + \frac{\partial u_j}{\partial x_i}\right) \tag{4}$$

Then, we introduce the fundamental solutions required in the MFS formulations. For two dimensions, Equation (1) can also be rewritten in matrix form as

$$\tilde{L}\begin{pmatrix} u_1 \\ u_2 \\ p \end{pmatrix} = \mathbf{0} \tag{5}$$

with

$$\tilde{L} = \begin{pmatrix} \mu(\nabla^2 - \lambda^2) & 0 & -\dfrac{\partial}{\partial x} \\ 0 & \mu(\nabla^2 - \lambda^2) & -\dfrac{\partial}{\partial y} \\ -\dfrac{\partial}{\partial x} & -\dfrac{\partial}{\partial y} & 0 \end{pmatrix} \tag{6}$$

where $1/\kappa=\lambda^2$.

The fundamental solutions of Equation (5) are defined by

$$\tilde{L}\begin{pmatrix} u_{11}^* & u_{12}^* & 0 \\ u_{21}^* & u_{22}^* & 0 \\ p_1^* & p_2^* & 0 \end{pmatrix} = \begin{pmatrix} -\delta(\mathbf{x}-\mathbf{s}) & 0 & 0 \\ 0 & -\delta(\mathbf{x}-\mathbf{s}) & 0 \\ 0 & 0 & 0 \end{pmatrix} \tag{7}$$

where $\mathbf{x}=(x_1, x_2)$, $\mathbf{s}=(s_1, s_2)$, and $\delta(\,)$ is the Dirac delta function. Equation (7) can be solved by using the Hörmander operator decomposition technique [23]. First of all, we introduce the adjoint

DOI: 10.1002/fld

operator of $\tilde{L}$ as

$$\tilde{L}^{\text{adj}} = \begin{pmatrix} -\dfrac{\partial^2}{\partial y^2} & \dfrac{\partial^2}{\partial x \partial y} & \mu \dfrac{\partial}{\partial x}(\nabla^2 - \lambda^2) \\ \dfrac{\partial^2}{\partial x \partial y} & -\dfrac{\partial^2}{\partial x^2} & \mu \dfrac{\partial}{\partial y}(\nabla^2 - \lambda^2) \\ \mu \dfrac{\partial}{\partial x}(\nabla^2 - \lambda^2) & \mu \dfrac{\partial}{\partial y}(\nabla^2 - \lambda^2) & \mu^2 (\nabla^2 - \lambda^2)^2 \end{pmatrix} \tag{8}$$

Then, we have

$$\tilde{L}\tilde{L}^{\text{adj}} = -\tilde{I}\mu\nabla^2(\nabla^2 - \lambda^2) \tag{9}$$

in which $\tilde{I}$ is the identity matrix. In the spirit of the Hörmander operator decomposition technique, we assume

$$\begin{pmatrix} u_{11}^* & u_{12}^* & 0 \\ u_{21}^* & u_{22}^* & 0 \\ p_1^* & p_2^* & 0 \end{pmatrix} = \frac{-1}{\mu} \tilde{L}^{\text{adj}} \begin{pmatrix} G & 0 & 0 \\ 0 & G & 0 \\ 0 & 0 & 0 \end{pmatrix} \tag{10}$$

By substituting Equation (10) into Equation (7) and using Equation (9), we have

$$\nabla^2(\nabla^2 - \lambda^2)G = -\delta(\mathbf{x} - \mathbf{s}) \tag{11}$$

The solution of Equation (11) can be found in the literature [24] as follows:

$$G = \frac{1}{2\pi\lambda^2}(K_0(\lambda|\mathbf{x} - \mathbf{s}|) + \log(|\mathbf{x} - \mathbf{s}|)) \tag{12}$$

where $K_n(\,)$ second kind modified Bessel function of order n. It should be noticed that Equation (12) can be selected up to homogeneous solutions. Consequently, we have the fundamental solutions of two-dimensional Brinkman equation by utilizing Equation (10) as follows:

$$u_{ik}^* = \frac{\delta_{ik}(-1 + \lambda r K_1(\lambda r) + \lambda^2 r^2 K_0(\lambda r))}{2\pi\lambda^2\mu r^2} + \frac{d_i d_k[2 - \lambda^2 r^2 K_2(\lambda r)]}{2\pi\lambda^2\mu r^4} \tag{13a}$$

$$p_k^* = \frac{d_k}{2\pi r^2} \tag{13b}$$

where r is the Euclidean distance between $\mathbf{x}$ and $\mathbf{s}$, and $d_i = x_i - s_i$. Then, the corresponding stress fundamental solutions can also be obtained by using the definition of Equation (4) as follows:

$$\sigma_{ijk}^* = \frac{\delta_{ij} d_k[4 - \lambda^2 r^2 - 2\lambda^2 r^2 K_2(\lambda r)]}{2\pi\lambda^2 r^4} + \frac{(\delta_{ik} d_j + \delta_{jk} d_i)[4 - 2\lambda^2 r^2 K_2(\lambda r) - \lambda^3 r^3 K_1(\lambda r)]}{2\pi\lambda^2 r^4} + \frac{d_i d_j d_k[-8 + \lambda^3 r^3 K_3(\lambda r)]}{\pi\lambda^2 r^6} \tag{14}$$

DOI: 10.1002/fld

where the following partial derivatives are supplied:

$$\frac{\partial u_{ik}^*}{\partial x_j} = \frac{\delta_{ik} d_j [2 - \lambda^2 r^2 K_2(\lambda r) - \lambda^3 r^3 K_1(\lambda r)]}{2\pi\lambda^2 \mu r^4} + \frac{(\delta_{ij} d_k + \delta_{jk} d_i)[2 - \lambda^2 r^2 K_2(\lambda r)]}{2\pi\lambda^2 \mu r^4} + \frac{d_i d_j d_k [-8 + \lambda^3 r^3 K_3(\lambda r)]}{2\pi\lambda^2 \mu r^6} \tag{15}$$

In Equations (13)–(15), $i, j, k = 1, 2$.

Similarly, we have the following results for three dimensions:

$$u_{ik}^* = \frac{\delta_{ik}[-1 + (1 + \lambda r + \lambda^2 r^2)\mathrm{e}^{-\lambda r}]}{4\pi\lambda^2 \mu r^3} + \frac{d_i d_k [3 - (3 + 3\lambda r + \lambda^2 r^2)\mathrm{e}^{-\lambda r}]}{4\pi\lambda^2 \mu r^5} \tag{16a}$$

$$p_k^* = \frac{d_k}{4\pi r^3} \tag{16b}$$

which are governed by

$$\begin{pmatrix} \mu(\nabla^2 - \lambda^2) & 0 & 0 & -\frac{\partial}{\partial x} \\ 0 & \mu(\nabla^2 - \lambda^2) & 0 & -\frac{\partial}{\partial y} \\ 0 & 0 & \mu(\nabla^2 - \lambda^2) & -\frac{\partial}{\partial z} \\ -\frac{\partial}{\partial x} & -\frac{\partial}{\partial y} & -\frac{\partial}{\partial z} & 0 \end{pmatrix} \begin{pmatrix} u_{11}^* & u_{12}^* & u_{13}^* & 0 \\ u_{21}^* & u_{22}^* & u_{23}^* & 0 \\ u_{31}^* & u_{32}^* & u_{33}^* & 0 \\ p_1^* & p_2^* & p_3^* & 0 \end{pmatrix} = \begin{pmatrix} -\delta(\mathbf{x} - \mathbf{s}) & 0 & 0 & 0 \\ 0 & -\delta(\mathbf{x} - \mathbf{s}) & 0 & 0 \\ 0 & 0 & -\delta(\mathbf{x} - \mathbf{s}) & 0 \\ 0 & 0 & 0 & 0 \end{pmatrix} \tag{17}$$

Also, we have the partial derivatives

$$\frac{\partial u_{ik}^*}{\partial x_j} = \frac{\delta_{ik} d_j [3 - (3 + 3\lambda r + 2\lambda^2 r^2 + \lambda^3 r^3)\mathrm{e}^{-\lambda r}]}{4\pi\lambda^2 \mu r^5} + \frac{(\delta_{ij} d_k + \delta_{jk} d_i)[3 - (3 + 3\lambda r + \lambda^2 r^2)\mathrm{e}^{-\lambda r}]}{4\pi\lambda^2 \mu r^5} + \frac{d_i d_j d_k [-15 + (15 + 15\lambda r + 6\lambda^2 r^2 + \lambda^3 r^3)\mathrm{e}^{-\lambda r}]}{4\pi\lambda^2 \mu r^7} \tag{18}$$

DOI: 10.1002/fld

and stresses

$$\sigma^*_{ijk} = \frac{\delta_{ij}d_k[6-\lambda^2r^2-(6+6\lambda r+2\lambda^2r^2)\mathrm{e}^{-\lambda r}]}{4\pi\lambda^2r^5} + \frac{(\delta_{ik}d_j+\delta_{jk}d_i)[6-(6+6\lambda r+3\lambda^2r^2+\lambda^3r^3)\mathrm{e}^{-\lambda r}]}{4\pi\lambda^2r^5} + \frac{d_id_jd_k[-15+(15+15\lambda r+6\lambda^2r^2+\lambda^3r^3)\mathrm{e}^{-\lambda r}]}{2\pi\lambda^2r^7} \tag{19}$$

In Equations (16)–(19), $i, j, k = 1, 2, 3$.

3. MFS FORMULATIONS

To demonstrate the MFS formulations, we take the three-dimensional cases as examples. By using the general theory of MFS [12, 13], the solution of Equations (1) and (2) can be represented arbitrarily well by

$$u_i(\mathbf{x}; \alpha_1^1, \ldots, \alpha_1^N, \alpha_2^1, \ldots, \alpha_2^N, \alpha_3^1, \ldots, \alpha_3^N, \mathbf{s}_1, \ldots, \mathbf{s}_N) \cong \sum_{k=1}^{3}\sum_{j=1}^{N} \alpha_k^j u_{ik}^*(\mathbf{x}, \mathbf{s}_j) \tag{20}$$

where $u_{ik}^*(\mathbf{x}, \mathbf{s}_j)$ is the fundamental solution given in Equation (16). Then, the corresponding traction can be obtained by using Equation (4) as follows:

$$t_i(\mathbf{x}; \alpha_1^1, \ldots, \alpha_1^N, \alpha_2^1, \ldots, \alpha_2^N, \alpha_3^1, \ldots, \alpha_3^N, \mathbf{s}_1, \ldots, \mathbf{s}_N) \cong \sum_{k=1}^{3}\sum_{j=1}^{N} \alpha_k^j t_{ik}^*(\mathbf{x}, \mathbf{s}_j) \tag{21}$$

with

$$t_{ik}^* = \sum_{j=1}^{3} \sigma_{ijk}^* n_j \tag{22}$$

where σ_{ijk}^* is given in Equation (19).

It is easily verified that Equation (20) satisfies the governing equations of Equation (1) analytically. Mathematically, Equation (20) is arbitrarily close to the solution if we have sufficient large number of source points. Numerically, boundary conditions in Equation (2) are simply collocated to determine the unknowns coordinates of source points $\mathbf{s}_j = (s_{j1}, s_{j2}, s_{j3})$ as well as the corresponding unknown intensities $\boldsymbol{\alpha}^j = (\alpha_1^j, \alpha_2^j, \alpha_3^j)$. Traditionally, the N source points $\mathbf{s}_j$ can be treated either as unknown or *a priori* known. In which the first case results in a nonlinear optimization with $6N$ unknowns, $\boldsymbol{\alpha}^j$ and $\mathbf{s}_j$. The solutions obtained by this way are highly accurate but procedure is more cumbersome [14]. On the other hand, if the source points are considered as *a priori* known, the boundary conditions are simply collocated at $N = N_1 + N_2$ boundary field points $\mathbf{x}_l$. It results in a linear equation system as follows:

$$\overline{u}_i(x_l) = \sum_{k=1}^{3}\sum_{j=1}^{N} \alpha_k^j u_{ik}^*(x_l, s_j) \quad \text{for } l = 1, 2, \ldots, N_1 \tag{23a}$$

DOI: 10.1002/fld

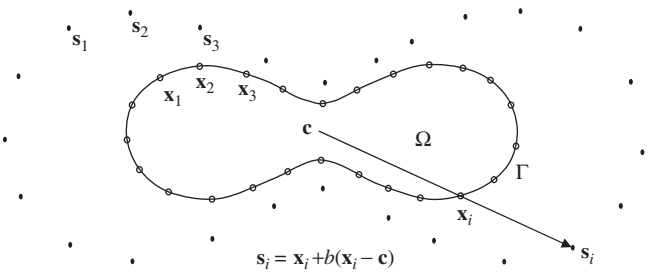

Figure 1. Schematic diagram of the source and field points.

$$\overline{t}_i(x_l) = \sum_{k=1}^{3} \sum_{j=1}^{N} \alpha_k^j t_{ik}^*(x_l, \mathbf{s}_j) \quad \text{for } l = N_1 + 1, N_1 + 2, \ldots, N_1 + N_2 \tag{23b}$$

In Equation (23), there are $3N$ equations with $3N$ unknowns, $\boldsymbol{\alpha}^j$, and thus can be solved. In this paper, we typically locate the boundary field points uniformly and place the source points stipulated out by a parameter of source location, b, as depicted in Figure 1. More details on the discussion of locating sources can be found in [25].

The MFS formulations for two dimensions are also similar and thus neglected here.

4. NUMERICAL RESULTS

In order to validate the proposed numerical method, the following four numerical experiments are considered: two-dimensional Dirchlet problem, two-dimensional Robin problem, three-dimensional Dirchlet problem, and three-dimensional Robin problem. The results are compared with their analytical values and the accuracies of the solutions obtained by the MFS are studied. Then, we applied the scheme to solve a peanut-shaped problem and a joint flow of Stokes and Brinkman fluids. In these examples, the root-mean-square error of the MFS is defined as

$$\sqrt{\frac{\sum_{j=1}^{\overline{N}} \sum_{i=1}^{\overline{L}} (u_{i,\text{numerical}}(\mathbf{x}_j) - u_{i,\text{exact}}(\mathbf{x}_j))^2}{\overline{L} \times \overline{N}}} \tag{24}$$

where $u_{i,\text{numerical}}(\mathbf{x}_j)$ is the numerical solutions obtained by the MFS (Equation (20)) at $\mathbf{x}_j$, $u_{i,\text{exact}}(\mathbf{x}_j)$ is the corresponding exact solution, $\overline{L}$ is the dimensionalities and $\overline{N}$ is the number of total nodes considered.

4.1. Two-dimensional Dirichlet problem

We consider the solutions of Equations (5) and (6) in a rectangle of 2×2 with center at $(0, 0)$ subjected to Dirchlet boundary conditions. The exact solution of the problem is

$$\begin{aligned} u_1 &= \cos x_1 \sinh x_2 \\ u_2 &= \sin x_1 \cosh x_2 \\ p &= -\lambda^2 \mu \sin x_1 \sinh x_2 \end{aligned} \tag{25}$$

DOI: 10.1002/fld

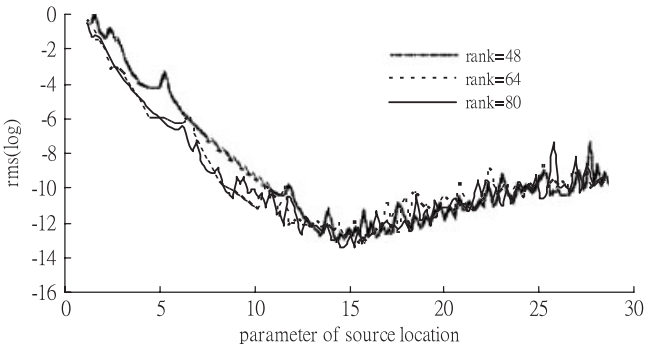

Figure 2. The errors of two-dimensional Dirchlet problem.

Furthermore, $\mu = 1$ and $\lambda = 3$ are selected typically. The exact solution of Equation (25) is obtained by assuming harmonic in x_1.

Figure 2 depicts the root-mean-square errors for different numbers of ranks and parameters of source location, in which the rank is associated to the matrix resulted from Equation (23). For two dimensions, the rank is two times the number of collocation nodes. From these results, it is observed that the MFS can obtain excellent solutions almost up to machine errors and generally farther sources result in better accuracy as predicted in theoretical articles [12, 13]. In addition, it is found that the errors are truncated if the parameters of source location exceed the capacity of equation solver. These are similar to the general works in [25].

4.2. Two-dimensional Robin problem

Then, we consider the rectangle subjected to the Neumann boundary condition at $x_1 = 1$ and Dirichlet boundary conditions elsewhere. The exact solution is the same as the previous case. Similarly, Figure 3 demonstrates the root-mean-square errors for different numbers of ranks and parameters of source location. Excellent results are also observed and they indicate that the MFS can easily be extended to Robin problems.

4.3. Three-dimensional Dirichlet problem

To validate the applicability of the proposed numerical method to three dimensions, we consider a cube of $2 \times 2 \times 2$ with center at $(0, 0, 0)$ subjected to Dirichlet boundary conditions. The exact solution of the problem is

$$\begin{aligned} u_1 &= \cos x_1 \sinh \frac{x_2 + x_3}{\sqrt{2}} \\ u_2 &= \frac{1}{\sqrt{2}} \sin x_1 \cosh \frac{x_2 + x_3}{\sqrt{2}} \\ u_3 &= \frac{1}{\sqrt{2}} \sin x_1 \cosh \frac{x_2 + x_3}{\sqrt{2}} \\ p &= -\lambda^2 \mu \sin x_1 \sinh \frac{x_2 + x_3}{\sqrt{2}} \end{aligned} \tag{26}$$

DOI: 10.1002/fld

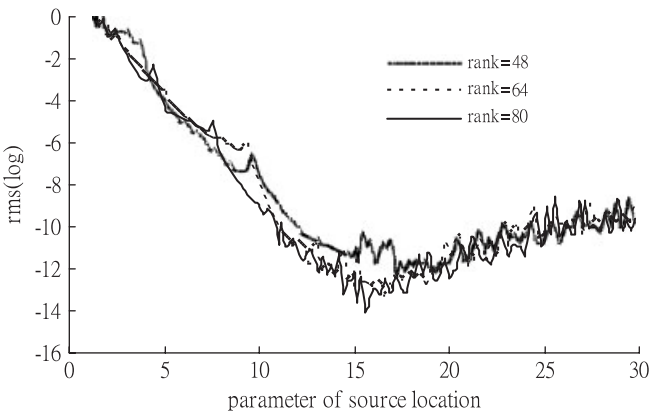

Figure 3. The errors of two-dimensional Robin problem.

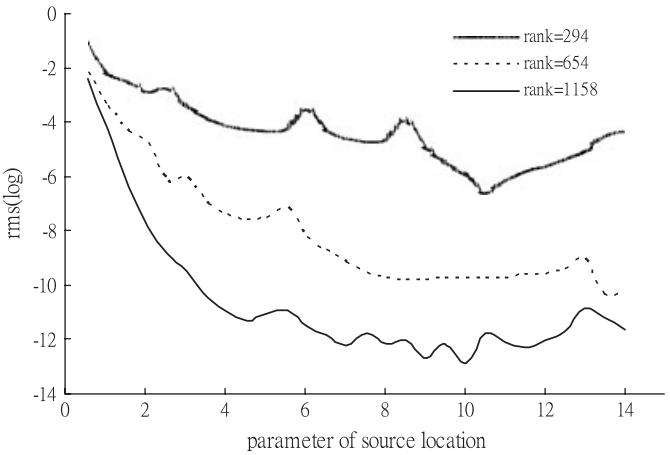

Figure 4. The errors of three-dimensional Dirchlet problem.

In the above, $\mu = 1$ and $\lambda = 1$ are assumed. The exact solution of Equation (26) is obtained by a rotation of Equation (25). The root-mean-square errors for different numbers of ranks and parameters of source location are described in Figure 4. For three dimensions, the rank is three times the number of collocation nodes. It is also observed from the figure that the solutions obtained by the MFS are in excellent agreements with the exact solutions.

4.4. Three-dimensional Robin problem

Then, we consider the cube subjected to the Neumann boundary condition at $x_1 = 1$ and Dirichlet boundary conditions elsewhere. The exact solution is the same as case III. Also, Figure 5 demonstrates the root-mean-square errors for this case. The excellent results indicate that the MFS also perform well for this three-dimensional Robin problem.

DOI: 10.1002/fld

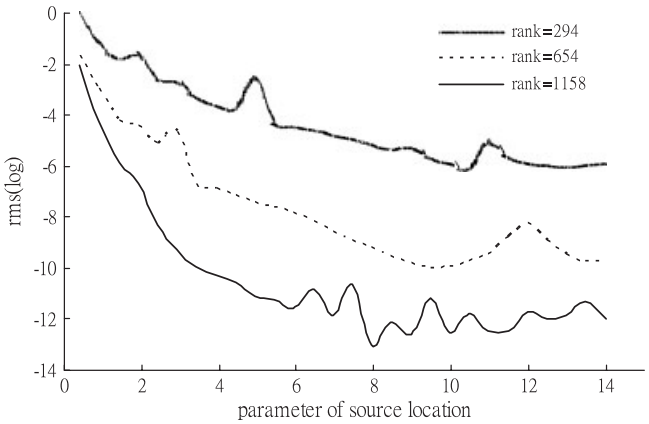

Figure 5. The errors of three-dimensional Robin problem.

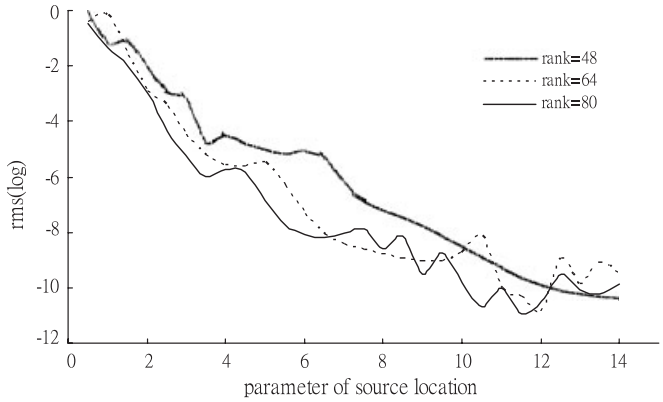

Figure 6. The errors of peanut-shaped problem.

4.5. Peanut-shaped problem

In order to demonstrate the flexibility of the MFS for irregular domains, two-dimensional peanut-shaped domain (Figure 1), defined by

$$r(\theta) = \sqrt{\cos 2\theta + \sqrt{1.1 - \sin^2 2\theta}}, \quad 0 \leqslant \theta \leqslant 2\pi \tag{27}$$

subjected to Dirichlet boundary condition is considered. In Equation (27), (r, θ) is the polar coordinate. The exact solution is set up by Equation (25). Figure 6 depicts the root-mean-square errors and excellent accuracies are also observed.

DOI: 10.1002/fld

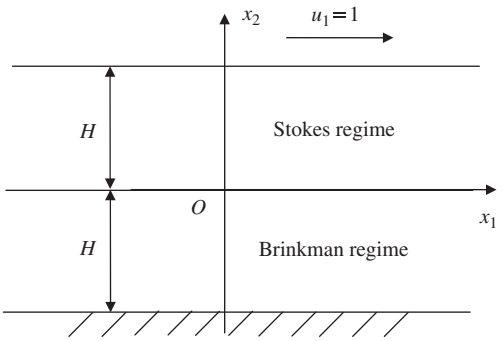

Figure 7. Geometric configuration of the application.

4.6. Application

When the MFS is applied to solve multi-phase problems or degenerate boundary value problems, the domain decomposition method (DDM) should be supplied [26]. As a final example, we consider a two-phase flow of Stokes and Brinkman fluids as depicted in Figure 7. The governing equations of the Stokes flows are

$$\begin{aligned} \nabla \cdot \mathbf{u} &= 0 \\ -\nabla p + \mu \nabla^2 \mathbf{u} &= 0 \end{aligned} \quad \text{in } \Omega \tag{28}$$

In addition, the MFS formulation for Stokes flows can be found in the literature [19, 20]. In these two articles, the traction kernels are not given explicitly, we supply them in tensor forms in Appendix. To form a single matrix, the MFS formulations for Stokes and Brinkman flows are collocated on the boundaries of $x_2>0$ and $x_2<0$, respectively. On the interface $x_2=0$, the connection conditions of continuous traction and velocity are imposed. Details of the combination of MFS and DDM can be found in the literature [26].

The exact solutions of the problem are

$$u_1 = \begin{cases} \dfrac{\tanh(\lambda H) + \lambda x_2}{\tanh(\lambda H) + \lambda H}, & x_2 \geqslant 0 \\ \dfrac{\tanh(\lambda H)\cosh(\lambda x_2) + \sinh(\lambda x_2)}{\tanh(\lambda H) + \lambda H}, & x_2 \leqslant 0 \end{cases} \tag{29a}$$

$$u_2 = 0 \tag{29b}$$

$$p = \text{constant} \tag{29c}$$

In our numerical experiments, $\lambda=3$, $H=1$ and $\mu=1$ in both regimes are set up. The root-mean-square errors are stated in Table I, which also perform well.

DOI: 10.1002/fld

Table I. The errors of the joint flow problem.

Rank	240	288	336	384
RMS	1.70E−09	7.43E−10	6.41E−10	4.33E−09

5. CONCLUSIONS

A numerical scheme of the MFS is developed for two- and three-dimensional slow Brinkman flows. The closed-form fundamental solutions, obtained by the Hörmander operator decomposition technique, their partial derivatives, the pressure, and the corresponding traction kernels are given explicitly in tensor forms. To validate the proposed numerical method, four numerical experiments of two and three dimensions with Dirichlet and Robin boundary conditions are carried out. Overall, the MFS can obtain excellent solutions almost up to machine errors. Then, the method is applied to a problem of peanut-shaped domain in two dimensions to demonstrate the flexibility of the proposed numerical method to treat irregular domains. Also, a joint flow of Stokes and Brinkman fluids is considered as an application. From these results, it is convinced that the MFS is a suitable meshless numerical method to solve slow Brinkman flows without integrations and singularities. Furthermore, these results also hint the possibility of further works on solving unsteady Stokes or even Navier–Stokes problems, if the dual reciprocity methods can be properly jointed.

APPENDIX

The two-dimensional fundamental solutions of Stokes flow, governed by Equation (7) with $\lambda = 0$, are

$$u_{ik}^* = -\frac{\delta_{ik}(2\ln r + 1)}{8\pi\mu} + \frac{d_i d_k}{4\pi\mu r^2} \tag{A1}$$

$$\frac{\partial u_{ik}^*}{\partial x_j} = -\frac{\delta_{ik} d_j}{4\pi\mu r^2} + \frac{(\delta_{ij} d_k + \delta_{jk} d_i)}{4\pi\mu r^2} - \frac{d_i d_j d_k}{2\pi\mu r^4} \tag{A2}$$

$$p_k^* = \frac{d_k}{2\pi r^2} \tag{A3}$$

$$\sigma_{ijk}^* = -\frac{d_i d_j d_k}{\pi r^4} \tag{A4}$$

It may be noticed that Equation (A1) is different from those in the literature [19, 20] since the fundamental solutions can be chosen up are to homogeneous solutions. Similarly, the three-dimensional fundamental solutions of Stokes flow, governed by Equation (17) with $\lambda = 0$, are

$$u_{ik}^* = \frac{\delta_{ik}}{8\pi\mu r} + \frac{d_i d_k}{8\pi\mu r^3} \tag{A5}$$

$$\frac{\partial u_{ik}^*}{\partial x_j} = -\frac{\delta_{ik} d_j}{8\pi\mu r^3} + \frac{(\delta_{ij} d_k + \delta_{jk} d_i)}{8\pi\mu r^3} - \frac{3 d_i d_j d_k}{8\pi\mu r^5} \tag{A6}$$

DOI: 10.1002/fld

$$p_k^* = \frac{d_k}{4\pi r^3} \tag{A7}$$

$$\sigma_{ijk}^* = -\frac{3d_i d_j d_k}{4\pi r^5} \tag{A8}$$

In Equations (A1)–(A4), $i, j, k = 1, 2$ and $i, j, k = 1, 2, 3$ in Equations (A5)–(A8).

ACKNOWLEDGEMENT

The support under Grant NSC 95-2221-E-464-002 by the National Science Council of Taiwan is gratefully acknowledged.

REFERENCES

1. Darcy H. *Les fontaines publique de la Ville de Dijon*. Victor Delmont: Paris, 1856.
2. Brinkman HC. A calculation of the viscous force exerted by a flowing fluid on a dense swarm of particles. *Applied Scientific Research A* 1947; **1**:27–34.
3. Kim S, Russel WB. The hydrodynamic interactions between two spheres in a Brinkman medium. *Journal of Fluid Mechanics* 1985; **154**:253–268.
4. Happel J. Viscous flow in multiparticle systems: slow motion of fluids relative to beds of spherical particles. *American Institute of Chemical Engineers Journal* 1958; **4**:197–201.
5. Masliyah JH, Neale G. Creeping flow over a composite sphere: solid core with porous shell. *Chemical Engineering Science* 1987; **42**:245–253.
6. O'Neill ME, Bhatt BS. Slow motion of a solid sphere in the presence of a naturally permeable surface. *Quarterly Journal of Mechanics and Applied Mathematics* 1991; **44**:91–104.
7. Tam CKW. The drag on a cloud of spherical particles in low Reynolds number flow. *Journal of Fluid Mechanics* 1969; **38**:537–546.
8. Lundgren TS. Slow flow through stationary random beds and suspensions of spheres. *Journal of Fluid Mechanics* 1972; **51**:273–299.
9. Howells ID. Drag due to the motion of a Newtonian fluid through a sparse random array of small fixed rigid objects. *Journal of Fluid Mechanics* 1974; **64**:449–475.
10. Misici L. Numerical solution of two transcendental equations. *Mathematics of Computation* 1984; **42**:589–595.
11. Kupradze VD, Aleksidze MA. The method of functional equations for the approximate solution of certain boundary value problems. *USSR Computational Mathematics and Mathematical Physics* 1964; **4**:82–126.
12. Mathon R, Johnston RL. The approximate solution of elliptic boundary-value problems by fundamental solutions. *SIAM Journal on Numerical Analysis* 1977; **14**:638–650.
13. Bogomolny A. Fundamental solutions method for elliptic boundary value problems. *SIAM Journal on Numerical Analysis* 1985; **22**:644–669.
14. Fairweather G, Karageorghis A. The method of fundamental solutions for elliptic boundary value problems. *Advances in Computational Mathematics* 1998; **9**:69–95.
15. Fairweather G, Karageorghis A, Martin PA. The method of fundamental solutions for scattering and radiation problems. *Engineering Analysis with Boundary Elements* 2003; **27**:759–769.
16. Tsai CC, Young DL, Chen CW, Fan CM. The method of fundamental solutions for eigenproblems in domains with and without interior holes. *Proceedings of the Royal Society of London, Series A* 2006; **462**:1443–1466.
17. Young DL, Tsai CC, Murugesan K, Fan CM, Chen CW. Time-dependent fundamental solutions for homogeneous diffusion problems. *Engineering Analysis with Boundary Elements* 2004; **28**:1463–1473.
18. Tsai CC, Young DL, Cheng AH-D. Meshless BEM for three-dimensional Stokes flows. *Computer Modeling in Engineering and Sciences* 2002; **3**:117–128.
19. Alves CJS, Silvestre AL. Density results using Stokeslets and a method of fundamental solution for the Stokes equations. *Engineering Analysis with Boundary Elements* 2004; **28**:1245–1252.
20. Tsai CC, Young DL, Lo DC, Wong TK. The method of fundamental solutions for three-dimensional Stokes flow in exterior field. *Journal of Engineering Mechanics* (ASCE) 2006; **132**:317–326.

DOI: 10.1002/fld

21. Golberg MA, Chen CS. The method of fundamental solutions for potential, Helmholtz and diffusion problems. In *Boundary Integral Methods*: *Numerical and Mathematical Aspects*, Golberg MA (ed.). Computational Mechanics Publications: Boston, 1998; 103–176.
22. Tsai CC, Young DL, Fan CM, Chen CW. MFS with time-dependent fundamental solutions for unsteady Stokes equations. *Engineering Analysis with Boundary Elements* 2006; **30**:897–908.
23. Hörmander H. *Linear Partial Differential Operators*. Springer: Berlin, 1963.
24. Cheng AH-D, Antes H, Ortner N. Fundamental solutions of products of Helmholtz and polyharmonic operators. *Engineering Analysis with Boundary Elements* 1994; **14**:187–191.
25. Tsai CC, Lin YC, Young DL, Atluri SN. Investigations on the accuracy and condition number for method of fundamental solutions. *Computer Modeling in Engineering and Sciences* 2006; **16**:103–114.
26. Chen CW, Fan CM, Young DL, Murugesan K, Tsai CC. Eigenanalysis of membranes with stringers by method of fundamental solutions and domain decomposition technique. *Computer Modeling in Engineering and Sciences* 2005; **8**:29–44.

DOI: 10.1002/fld